$CD8^+$ T cells specific for a malaria cytoplasmic antigen form clusters around infected hepatocytes and are protective at the liver stage of infection

Running title: $CD8^+$ T cell recognition of cytoplasmic malaria antigen

Kazumi Kimura[1], Daisuke Kimura[1], Yoshifumi Matsushima[1],

Mana Miyakoda[1], Kiri Honma[1], Masao Yuda[3], Katsuyuki Yui[1,2,#]

[1]Division of Immunology, Department of Molecular Microbiology and Immunology, Nagasaki University, Graduate School of Biomedical Sciences, 1-12-4, Sakamoto, Nagasaki, 852-8523 Japan; [2]Global COE programs, Nagasaki University, 1-12-4, Sakamoto, Nagasaki, 852-8523 Japan; [3]Department of Medical Zoology, School of Medicine, Mie University, 2-174, Edobashi, Tsu, 514-8507 Japan

#Corresponding author: Katsuyuki Yui, Division of Immunology, Department of Molecular Microbiology and Immunology, Graduate School of Biomedical Sciences, Nagasaki University, 1-12-4, Sakamoto, Nagasaki 852-8523, Japan.

TEL: +81-95-819-7070; FAX: +81-95-819-7073; E-mail: katsu@nagasaki-u.ac.jp

ABSTRACT

Following *Anopheles* mosquito-mediated introduction into a human host, *Plasmodium* parasites infect hepatocytes and undergo intensive replication. Accumulating evidence indicates that $CD8^+$ T cells induced by immunization with attenuated *Plasmodium* sporozoites can confer sterile immunity at the liver stage of infection; however, the mechanisms underlying this protection are not clearly understood. To address this, we generated recombinant *Plasmodium berghei* ANKA expressing a fusion protein of an ovalbumin epitope and green fluorescent protein in the cytoplasm of the parasite. We have shown that the ovalbumin epitope is presented by infected liver cells in a transporter associated with antigen processing–dependent manner and becomes a target of specific $CD8^+$ T cells (OT-I cells), leading to protection at the liver stage of *Plasmodium* infection. We visualized the interaction between OT-I cells and infected hepatocytes by intravital imaging using two-photon microscopy. OT-I cells formed clusters around infected hepatocytes, leading to the elimination of the intra-hepatic parasites and subsequent formation of large clusters of OT-I cells in the liver. Interferon-γ expressed in $CD8^+$ T cells was dispensable for this protective response. Additionally, we found that polyclonal

ovalbumin-specific memory $CD8^+$ T cells induced by *de novo* immunization were able to confer sterile protection, although the threshold frequency of the protection was relatively high. These studies revealed a novel mechanism of specific $CD8^+$ T cell-mediated protective immunity, and demonstrated that proteins expressed in the cytoplasm of *Plasmodium* parasites can become targets of specific $CD8^+$ T cells during liver-stage infection.

INTRODUCTION

Plasmodium sporozoites are transmitted by the bites of *Anopheles* mosquitoes under the skin and are transported via the bloodstream to the liver, where they infect hepatocytes. Immunization with irradiated sporozoites can induce sterile protection at pre-erythrocytic stages of infection in both mice and humans (1-3). Similarly, sterile protective immunity is induced by *Plasmodium* parasites that have been genetically attenuated by a gene deletion and which arrest at the hepatic stage (4, 5). Recent studies have shown that the infection of mice under chloroquine shield induces a protective immune response at the hepatic stage of infection (6). Immunization by these methods induces multiple different mechanisms of protection involving $CD8^+$ T cells, $CD4^+$ T cells, B cells, and NK cells (7, 8). Among the major effector cells are $CD8^+$ T cells, which recognize malaria antigen in association with major histocompatibility complex (MHC) class I during liver-stage infection (9)

Targets for protective immunity against malaria were identified using antibodies obtained from mice immunized with irradiated sporozoites, including circumsporozoite protein

(CSP), which was extensively investigated (10, 11). CSP is expressed on the surface of sporozoites and liver-stage malaria parasites and is the most advanced target antigen of liver-stage vaccine development. The major liver-stage effector cells specific for CSP are $CD8^+$ T cells, as shown by the depletion of $CD8^+$ T cells with the antibody abrogating protection and by the resistance to subsequent challenge infection conferred by cloned specific T cells. Further studies using CSP-transgenic mice indicated that additional protective antigens are present, although CSP is the major antigen that can induce protection against pre-erythrocytic forms of malaria in BALB/c mice (12). Additional candidate antigens at the liver stage of infection include sporozoite surface protein 2 (SSP), which was identified using an antibody produced by BALB/c mice after immunization with irradiated sporozoites, and which induces protection that is mediated by $CD8^+$ T cells, $CD4^+$ T cells, and antibodies (13-15). Protective immunity via immunization is much more difficult to establish in C57BL/6 (B6) mice than in BALB/c mice, partly because the H-2^b-restricted cytotoxic T lymphocyte (CTL) epitope is not present in CSP (16). However, protection is induced in B6 mice by immunization with attenuated *Plasmodium* parasites or infection under a chloroquine shield. This protective

73 immunity is also mediated by $CD8^+$ T cells, whose target antigen is not CSP. These latter
74 studies suggest the existence of unknown target antigens recognized by $CD8^+$ T cells in
75 infected hepatocytes, in addition to CSP and SSP2.
76
77 Research efforts are in progress to identify novel malaria antigen targets expressed at the
78 liver stage. Genome-wide expression profiling studies have indicated that many malaria
79 proteins are expressed during liver-stage infection (17, 18). However, the criteria that
80 would frame the search for target malaria antigens have not yet been established. Several
81 studies have suggested that the localization of antigen within microbial pathogens is
82 important for the generation of specific T cells and the resulting protection. It is generally
83 thought that secreted antigens are more accessible to antigen presentation pathways and
84 induce strong T cell immune responses (19). For example, intracellular bacteria such as
85 *Mycobacterium tuberculosis* remain in the phagosome, where they survive and replicate.
86 The secreted form of the antigens expressed in these bacteria can be presented via the
87 MHC I pathway, through a process that appears to be facilitated by an increase in
88 permeability of the endosomal membrane by the microbe (20, 21). In an infection model

89 using recombinant *Trypanosoma cruzi* expressing an ovalbumin (OVA) epitope, it was
90 shown that host cells were able to present OVA via the MHC I pathway when the antigen
91 was produced in secretory form, but not the cytoplasmic or transmembrane form (22). It
92 has also been proposed that CSP is released from the surface of sporozoites directly into
93 the cytoplasm of host hepatocytes, where it binds to RNA-associated host cell targets (23,
94 24). Furthermore, CSP is released from the surface of sporozoites when they travel
95 through hepatocytes before reaching the final infected hepatocyte, and appears to be
96 presented by these traversed hepatocytes to specific T cells (25). Therefore, the search
97 for candidate malaria antigens for liver-stage infection is generally focused on molecules
98 expressed on the surface of parasites. However, it is not clear whether intracytoplasmic
99 molecules are able to become targets of the protective immune responses during
100 liver-stage infection.
101
102 In this study, we generated recombinant parasites that exhibited cytoplasmic expression
103 of an OVA epitope presented by MHC I. We examined whether this epitope was
104 presented by infected hepatocytes and whether it became a target of specific OT-I $CD8^+$ T

105 cells leading to protection at the liver stage of infection. We also examined the

106 mechanisms underlying the presentation of this antigen and visualized the interaction of

107 OT-I cells with infected hepatocytes by intravital imaging using two-photon microscopy

108 (TPM). The results of these experiments suggest that $CD8^+$ T cells can recognize

109 cytoplasmic malaria antigens, form clusters around infected hepatocytes, and protect

110 against parasites.

MATERIALS AND METHODS

Parasites

Recombinant *P. berghei* ANKA (PbA) expressing class II and class I OVA epitopes fused to the N- and C-terminus of a *P. yoelii* hsp70 fragment (PbA-hsOVA), respectively, and *P. berghei* ANKA expressing OVA class I epitope fused to the C-terminus of green fluorescent protein (GFP) (PbA-gfpOVA) were constructed as previously described (26) (Fig. 1A). PbA-hsOVA expresses a recombinant fusion protein containing the N-terminal sequence (aa 1–5) of *P. berghei* hsp70, an $OVA_{323-339}$ MHC II epitope, a truncated sequence (aa 201–398) of *P. yoelii* hsp70, and an $OVA_{257-264}$ MHC I epitope. PbA-gfpOVA express a protein containing an $OVA_{257-264}$ MHC I epitope fused to the C-terminus of GFP. After transfection, mice were infected and were maintained under the presence of the anti-malaria drug pyrimethamin. PbA-gfpOVA were enriched by sorting of GFP-positive erythrocytes using FACSAria (BD Biosciences, San Jose, CA). The stable transfectant was cloned by limiting dilution in mice and was maintained by alternating passage between *Anopheles stephensi* and BALB/c mice. Sporozoites were prepared from salivary glands of *A. stephensi* after 18–24 days of infection with

PbA-hsOVA or PbA-gfpOVA.

Animals

OT-I and OT-II transgenic mice expressing the T cell receptor (TCR) specific for $OVA_{257-264}$/ K^b and $OVA_{323-339}/IA^b$, respectively, were provided by Dr. H. Kosaka (Osaka University, Osaka, Japan) (27, 28). $TAP^{-/-}$ mice (B6 background) were provided by Dr. H. Watanabe (Ryukyu University, Okinawa, Japan) (29). B6.SJL and OT-I or OT-II mice were interbred, and the offspring were intercrossed to obtain $CD45.1^+$ OT-I or OT-II mice. DsRed transgenic, IFN-$\gamma^{-/-}$ and perforin$^{-/-}$ mice were purchased from The Jackson Laboratory (Bar Harbor, ME). DsRed transgenic mice and OT-I mice were crossed to produce DsRed/OT-I mice. OT-I and IFN-$\gamma^{-/-}$ or perforin$^{-/-}$ mice were bred to produce IFN-$\gamma^{-/-}$ OT-I mice, perforin$^{-/-}$ OT-I mice, and IFN-$\gamma^{-/-}$perforin$^{-/-}$ OT-I mice. B6 and BALB/c mice were purchased from SLC (Shizuoka, Japan). Mice were maintained in the Laboratory Animal Center for Animal Research at Nagasaki University and were used at the age of 8–14 wks. To generate bone marrow chimeras, B6 or $TAP^{-/-}$ mice were lethally irradiated (900 rad) and received bone marrow cells (1.0×10^7; prepared from

143 $TAP^{-/-}$ or B6 mice) intravenously on the following day. Mice were left for at least two

144 months before infection to allow for reconstitution of the lymphoid system. The animal

145 experiments reported herein were approved by the Institutional Animal Care and Use

146 Committee of Nagasaki University and were conducted according to the guidelines for

147 Animal Experimentation at Nagasaki University.

148

149 Adoptive transfer and PbA infection

150 To prepare activated OT-I cells, pooled cells from the spleen and inguinal lymph nodes of

151 OT-I mice were prepared and cultured in the presence of $OVA_{257-264}$ peptide (2 μg/ml) for

152 3 days. OT-II cells were purified from spleen and inguinal lymph node cells of OT-II

153 mice using anti-CD4 IMag (BD Biosciences). Dendritic cells were prepared from B6

154 splenocytes using CD11c-microbeads and AutoMACS (Myltenyi Biotec, Bergisch

155 Gladbach, Germany). OT-II (6×10^6/ml) and dendritic cells (1×10^5/ml) were

156 co-cultured in the presence of $OVA_{323-339}$ peptide (3 μ g/ml) for 5 days. Mice received

157 OT-I ($1–100 \times 10^5$) or OT-II (3×10^7) cells through the tail vein, and were challenged

158 with 300–500 infectious sporozoites 2 days later. The proportion of OT-I (CD45.1) cells

159 in the total $CD8^+$ T cell population was determined by staining peripheral blood
160 lymphocytes (PBLs) with APC-anti-CD8 and PECy7-anti-CD45.1 mAbs. For the
161 experiments involving *de novo* priming of $CD8^+$ T cells (Fig. 6) and parasite burden in the
162 liver (Fig. 3), mice were challenged with 1,000 and 5,000 sporozoites, respectively. Mice
163 were monitored for parasitemia daily (starting 4 days after infection) by microscopic
164 examination of standard blood films. Parasite burden was determined by real-time PCR
165 using liver RNA and is expressed as a ratio of the cDNA of *Plasmodium* 18S rRNA to
166 cDNA of mouse G3PDH, as described previously (30).
167
168 **Confocal and two-photon microscopy**
169 PbA-gfpOVA sporozoites were obtained from the salivary glands of infected *A. stephensi*
170 mosquitoes. To prepare PbA-infected hepatocytes, HepG2 cells (1×10^4) were cultured
171 in HepG2 medium (500 μL; DMEM containing 10% fetal calf serum, 1%
172 penicillin/streptomycin, and 1% non-essential amino acids) using Fluorodish (World
173 Precision Instruments, Sarasota, FL) for 3 days as described previously (31).
174 PbA-gfpOVA sporozoites (1×10^4) were added to the culture and incubated for 3 h,

175 followed by the addition of invasion medium (500 μL; HepG2 medium supplemented
176 with 3 mg/ml of glucose). The medium was replaced 12 h later, and the culture was
177 maintained for a total of 24 h in the invasion medium, after which cells were stained.
178 PbA-gfpOVA-infected red blood cells (RBCs) were collected from the tail vein of the
179 infected mice. Sporozoites, infected HepG2 cells, and RBCs were incubated in the
180 presence of Bodipy-TR-C_5-ceratide (5 μM, Invitrogen, Carlsbad, CA) for 15 min at
181 37°C, washed 3 times with PBS, and stained with DRAQ5 (1.25 μM, Biostatus,
182 Leicestershire, UK) for 30 min at 37°C. Images were acquired with an inverted TCS SP5
183 MP confocal microscope with a 63× glycerol immersion lens (Leica Microsystems,
184 Wetzlar, Germany).
185
186 For intravital imaging, spleen cells and lymph node cells from DsRed/OT-I mice were
187 cultured in the presence of $OVA_{257-264}$ for 3 days. Activated DsRed/OT-I cells (3–10 ×
188 10^6) were adoptively transferred into B6 mice. Two days later, the mice were infected (or
189 not infected, for controls) with PbA-gfpOVA sporozoites (1×10^4). At 40–48 h
190 post-infection, mice were anesthetized with isoflurane. The abdomen was then shaved

and a midline incision was made through the dermis and peritoneum and the liver was carefully exteriorized. Mice were placed on a platform with a centrally located hole, where a cover glass was attached. An O-ring with a 9.8 mm inner diameter was placed on the cover glass to prevent movement of the liver during imaging. Images were acquired with an inverted TCS SP5 TPM microscope equipped with an OPO laser (Leica Microsystems) and with a 25 × 0.95NA water immersion objective. During observation with fluorescence microscopy (DMI6000B, Leica Microsystems), the numbers of GFP^+ infected hepatocytes and OT-I clusters were determined by counting manually within the field inside the O-ring (~75 mm^2). The number of OT-I cells in each cluster was determined using Imaris software (Bitplane, Zurich, Switzerland) after acquiring a 3 dimensional image of each cluster with TPM.

Generation of OVA-specific memory $CD8^+$ T cells

Specific memory $CD8^+$ T cells were induced in mice as described previously (32) with slight modifications. B6 mice were immunized intravenously with bone marrow-derived dendritic cells (2.5×10^5) pulsed with $OVA_{257-264}$ peptide (1 mM). Seven to 9 days later,

these mice were boosted by infection with *Listeria monocytogenes* expressing OVA (LM-OVA; 1–10 × 10^6 CFU) (33). After 2 months, PBLs from these mice were stained with FITC-anti-CD8 mAb and PE-$OVA_{257-264}$ /H-$2K^b$ tetramer (MBL, Nagoya, Japan), and the proportion of OVA-specific $CD8^+$ T cells was determined using FACS Canto II (BD Biosciences).

Statistical Analysis

Data are expressed as means ± standard deviation (SD). Statistical analysis was performed using the Mann-Whitney *U* test for the comparison of two experimental groups, and the data were analyzed using GraphPad Prism software. Differences with a p value of < 0.05 were considered significant.

RESULTS

Cytoplasmic expression of OVA-GFP fusion proteins in recombinant PbA

To investigate the mechanisms of protection against liver-stage malaria, we generated two recombinant PbA constructs (Fig. 1A). The first construct expresses a fusion protein of the $OVA_{257-264}$ epitope fused to the C-terminus of GFP (PbA-gfpOVA); the second expresses a fusion protein of the $OVA_{323-339}$ MHC II epitope, a portion of *P. yoelii* hsp70, and the $OVA_{257-264}$ MHC I epitope (PbA-hsOVA). The sequence of *P. yoelii* hsp70 was used because an antigen fused to this portion of hsp70 was shown to promote priming of specific T cell responses (34, 35). Since the fusion protein constructs did not contain a signal sequence, its expression was expected to be limited to the cytoplasm of the parasite. To confirm the localization of the expressed protein, confocal microscopy was used to examine the expression of the fusion protein in sporozoites and infected cells after staining with membrane marker bodipy-TR-C_5-ceramide and nuclear marker DRAQ5 (36) (Fig. 1B). The GFP-fused protein was localized in the cytoplasm of PbA-gfpOVA sporozoites. At 24 h post-infection with sporozoites, GFP protein was detected within the parasitophorous membrane of the infected HepG2 cells, but was not observed in the host

235 cytoplasm. We also examined the expression of GFP in the infected RBCs, and observed
236 that GFP was also localized within the parasitophorous membrane in these cells.
237
238 **OT-I cell-mediated protection against liver-stage infection with PbA**
239 We examined whether $CD8^+$ T cells from OT-I mice are protective against liver-stage
240 infection with PbA-hsOVA and PbA-gfpOVA. OT-I cells were activated prior to transfer,
241 since previous studies indicated that the activation of specific $CD8^+$ T cells was required
242 for protection against sporozoite infection at the liver stage (37). B6 mice were
243 inoculated with different doses of preactivated OT-I cells and then infected with
244 PbA-hsOVA or wild-type PbA sporozoites, and the levels of parasitemia were monitored
245 daily (Fig. 2A). Transferred OT-I cells were identified as $CD45.1^+CD8^{low}$ T cells (38).
246 Mice that received 1×10^7 OT-I cells were completely protected from challenge infection
247 with PbA-hsOVA but not with PbA, indicating that the protective effect was specific to
248 the OVA-expressing parasites. We also observed that the protection was OT-I dose
249 dependent, and that mice receiving less than 1×10^6 OT-I cells developed parasitemia
250 (Fig. 2A). OT-I cells constituted 42.1% and 3.4% of the $CD8^+$ T cell population in PBL

from mice receiving 1×10^7 and 1×10^6 OT-I cells, respectively, indicating that high levels of OT-I cells were required for sterile protection at the liver stage of infection. Similarly, sterile protection was observed when mice receiving OT-I cells were infected with PbA-gfpOVA sporozoites (Fig. 2B). We also examined whether $CD4^+$ T cells from OT-II mice were protective against the liver-stage infection with PbA-hsOVA (Fig 2C). Although parasitemia appeared 5 days after infection in both mice transferred and not transferred with OT-II, the levels of parasitemia were lower in the OT-II-transferred mice, suggesting that OT-II cells have protective roles against infection with PbA-hsOVA. However, sterile immunity was never achieved at the liver stage by inoculation with OT-II cells, although the proportion of OT-II cells in the $CD4^+$ T cell population was as high as 43.8%.

To confirm that the observed decrease in parasitemia was due to the inhibition of parasite growth at the liver stage, parasite burden in the liver was examined by real-time PCR of parasite ribosomal RNA (Fig. 3A). OT-I cells were found to significantly inhibit the parasite burden in the liver of mice infected with PbA-hsOVA (90.1% reduction), but not

267 with PbA, indicating that the protection was specific to the OVA-expressing PbA. We
268 next wanted to examine whether the OVA antigen-presenting pathway utilizes the
269 classical MHC class I pathway. To this end, B6 and $TAP^{-/-}$ mice were inoculated with
270 OT-I cells, infected with PbA-hsOVA, and examined for parasite burden in the liver. OT-I
271 cells significantly inhibited the parasite burden in B6 mice (99.8% reduction), but not in
272 $TAP^{-/-}$ mice after challenge infection with PbA-hsOVA sporozoites, indicating that the
273 antigen presentation pathway did utilize the classical TAP-dependent pathway (Fig. 3B).
274 Furthermore, we generated bone marrow chimeras between B6 and $TAP^{-/-}$ mice to
275 examine whether TAP expressed in hematopoietic cells or hepatocytes is critical for the
276 protection. After inoculation with OT-I and infection with PbA-hsOVA, the parasite
277 burden in the liver was significantly reduced in bone marrow chimeras when B6 mice
278 were used as recipients. The reductions were 98.2% in the B6 → B6 chimera compared
279 to B6 → $TAP^{-/-}$, and 98.1% in the $TAP^{-/-}$ → B6 chimera compared to $TAP^{-/-}$ → $TAP^{-/-}$,
280 indicating that TAP expression in the radioresistant host is critical for the protection
281 against challenge infection with PbA-hsOVA (Fig. 3C). These results strongly suggest
282 that hepatocytes infected with PbA-hsOVA sporozoites process and present the OVA

283 epitope via the classical MHC class I pathway, which is consistent with a previous study
284 using *P. berghei* expressing a mutant CS protein containing an OVA epitope (39).
285
286 ***In vivo* imaging of the interaction between OT-I cells and infected hepatocytes**
287 After observing the protective effect of OT-I cells, we aimed to directly visualize the
288 interaction of infected hepatocytes with the effector OT-I cells using TPM. For this
289 purpose, mice were inoculated (or not inoculated, for controls) with pre-activated
290 DsRed/OT-I cells and infected with PbA-gfpOVA sporozoites. Two days later, the livers
291 of the infected mice were surgically exposed and imaging was performed. In mice
292 infected with PbA-gfpOVA sporozoites, GFP^+ cells were clearly visible after 24 h and the
293 quantity of GFP continued to increase for 24–48 h after infection (data not shown). We
294 observed a defined surface area (75 mm^2) of the liver using TPM at 40–48 h after
295 sporozoite infection. When a low dose (3×10^6) of OT-I cells was inoculated into the
296 mice, we observed numerous OT-I clusters formed around GFP^+ cells (Fig. 4A). The
297 number of OT-I cells in each of these clusters was relatively small (mean 34.2, range
298 10–71) (Fig. 4D GFP+). Using time-lapse imaging, we were able to observe the

299 disappearance of GFP^+ cells while in contact with OT-I cells, suggesting that the OT-I
300 cells are directly involved in the elimination of intra-hepatic parasites (Fig. 4A right,
301 supplementary Fig. 1). When the number of inoculated OT-I cells was increased to the
302 dose sufficient for sterile protection (1×10^7), fewer GFP^+ cells remained in the liver (Fig.
303 4B, C left panel), and the number of OT-I clusters increased (Fig. 4B, C right panel). The
304 number of OT-I clusters in the liver of the OT-I-inoculated, PbA-infected mice was
305 similar to the number of GFP^+ cells in the PbA-infected mice without OT-I-inoculation,
306 suggesting that the clusters were formed following elimination of infected hepatocytes by
307 OT-I cells (compare the left and right panels of Fig. 4E). Additionally, we determined
308 that the number of OT-I cells in clusters containing GFP^+ cells (mean 28.4, range 14–48)
309 was much lower than in clusters that did not contain GFP^+ cells (mean 293.8, range 15-
310 –1,415) in mice inoculated with 1×10^7 OT-I cells (Fig 4D). The OT-I clusters were
311 barely detectable in OT-I-inoculated mice without PbA infection and, if present, were
312 formed by small numbers of OT-I cells (Fig. 4E right panel, F).
313
314 **Effector function of OT-I cells**

315 The clustering of OT-I cells around infected hepatocytes suggests that the effector
316 mechanisms of $CD8^+$ T cells in liver-stage malaria might be different from the classical
317 CTL killing mechanisms. Thus, we evaluated the effector function of $CD8^+$ T cells
318 during protection at the liver stage of infection with PbA-hsOVA or PbA-gfpOVA. $CD8^+$
319 T cells were prepared from OT-I, IFN-$\gamma^{-/-}$ OT-I, perforin$^{-/-}$ OT-I, or IFN-$\gamma^{-/-}$ perforin$^{-/-}$ OT-I
320 mice, activated *in vitro*, and transferred into B6 mice, which were infected with
321 sporozoites of PbA-hsOVA or PbA-gfpOVA and examined for parasitemia (Fig. 5). After
322 infection with PbA-hsOVA, no parasitemia was detected in mice receiving IFN-$\gamma^{-/-}$ OT-I,
323 perforin$^{-/-}$ OT-I, or IFN-$\gamma^{-/-}$ perforin$^{-/-}$ OT-I cells, indicating that the expression of IFN-γ
324 and perforin in $CD8^+$ T cells was dispensable for the protection against liver-stage
325 infection (Fig. 5A). When the mice were infected with PbA-gfpOVA, a delayed onset of
326 parasitemia was detected in 2/5 infected mice receiving transferred IFN-$\gamma^{-/-}$ perforin$^{-/-}$
327 OT-I cells, and 1/5 mice receiving perforin$^{-/-}$ OT-I cells (Fig 5B). These results suggest
328 that IFN-γ and perforin are partially involved in the protective effects of OT-I cells,
329 although these molecules are not essential for protection. The difference in the results of
330 infection with PbA-hsOVA and PbA-gfpOVA may be due to the differences in the

331 efficiency of antigen presentation; the OVA epitope may be more efficiently presented to
332 OT-I cells for PbA-hsOVA infection than for PbA-gfpOVA infection.
333
334 Finally, we examined whether OVA-specific polyclonal memory $CD8^+$ T cells were
335 protective against infection with PbA-hsOVA sporozoites following a previously
336 described protocol (40). Mice were primed with $OVA_{257-264}$-pulsed dendritic cells and
337 boosted with LM-OVA infection. Two months later, we examined the proportion of
338 OVA-specific $CD8^+$ T cells in PBL by staining with OVA/K^b tetramer. These mice were
339 infected with PbA-hsOVA sporozoites, and the levels of parasitemia in peripheral blood
340 were determined 8 days after infection (Fig. 6). Comparison of the number of
341 tetramer-positive cells with the occurrence of parasitemia showed that mice bearing
342 OVA-specific $CD8^+$ T cells at levels more than 9.31% of total $CD8^+$ T cells were
343 completely protected from the sporozoite challenge, while those bearing specific $CD8^+$ T
344 cells in the range of 1.1–8.8% included both protected and unprotected mice.
345

DISCUSSION

In this study, we established a novel system to investigate the cellular and molecular mechanisms underlying the protective immune response against liver-stage infection with malaria parasites using a model malaria antigen, OVA. Unlike the CSP model, which utilizes BALB/c mice, our model can be applied in B6 mice. Cockburn et al. generated a model in which CS protein containing an OVA epitope was expressed on the surface of sporozoites, and used B6 mice for the study of protective immunity at the liver stage of infection (39). Our model is distinct from this model in that the antigen is expressed in the cytoplasm of malaria parasites, and can become a target of specific $CD8^+$ T cells during the liver stage of *Plasmodium* infection, leading to sterile protection. Protection was achieved by both the inoculation of activated OT-I cells and by the induction of polyclonal OVA-specific memory $CD8^+$ T cells. Since protection by OT-I cells was dependent on TAP molecule expression in non-hematopoietic host cells, consistent with the previous study (39), it is reasonable to speculate that OVA expressed in the cytoplasm of the parasite is somehow transported into the cytoplasm of hepatocytes for antigen processing. However, we did not detect any leakage of GFP into the

362 cytoplasm of the infected hepatocytes by confocal imaging. A possible explanation for
363 this is that cytoplasmic malaria antigens are processed to smaller peptides prior to transfer
364 into the host cells. Alternatively, the amount of the protein transported to the cytoplasm
365 may have been too low for visualization by our methods. Whatever the molecular
366 mechanisms, these results imply that malaria proteins expressed in the cytoplasm of
367 malaria parasites can be targets of protective immune responses, and should not be
368 excluded from the pool of candidate malaria vaccine targets.
369
370 In our experimental model, we employed intravital imaging to visualize the interaction
371 between PbA-infected hepatocytes and specific $CD8^+$ T cells. In the absence of
372 inoculation with OT-I cells, infected hepatocytes were observed as isolated GFP^+ cells, as
373 shown previously by others (41-43). When we used a lower number of OT-I cells for
374 inoculation (3×10^6), clustering of OT-I cells around the infected hepatocytes was
375 observed, suggesting that OT-I cells recognize the MHC/OVA epitope expressed on the
376 surface of hepatocytes, and make direct contacts with them. Using time-lapse imaging,
377 we were able to observe the disappearance of GFP^+ intra-hepatic parasites during their

interaction with OT-I cells, implying that the OT-I clusters are directly involved in the elimination of the parasites in the liver. When the number of inoculated OT-I cells was increased to a level sufficient for sterile immunity (1×10^7), the number of GFP^+ cells was dramatically reduced. Furthermore, we observed OT-I clusters that did not contain GFP^+ hepatocytes, and some OT-I clusters were large (containing more than 1,000 OT-I cells), suggesting that the accumulation of OT-I cells in the cluster continued after the elimination of GFP^+ hepatocytes. After the submission of this manuscript, Cockburn et al. (44) published an imaging study of CSP-specific $CD8^+$ T cells eliminating liver-stage malaria parasites, and showed that $CD8^+$ T cells form clusters around infected hepatocytes, similar to our study. Thus, cluster formation is not limited to our model system, but occurs in *Plasmodium*-specific $CD8^+$ T cells eliminating malaria parasites during liver-stage infection.

The effector mechanisms of $CD8^+$ T cell-mediated elimination of intra-hepatic parasites are complex. An earlier study suggested that perforin- or Fas-mediated killing is not the main pathway of parasite elimination during the hepatic stage of the infection (45).

394 Additionally, a recent study using CSP-specific transgenic T cells suggested that IFN-γ is
395 not essential for the protection of mice against infection with *P. yoelii* sporozoites (46).
396 However, IFN-γ and TNF-α have been reported to be important for the protection against
397 liver-stage infection with *P. berghei* as well as *P. yoelii*, while perforin is important for
398 protection against infection with *P. yoelii* but not *P. berghei* (47, 48). In our study, IFN-γ
399 expressed in $CD8^+$ T cells was dispensable for in the elimination of infected hepatocytes
400 during infection with PbA-gfpOVA, whereas perforin was partially involved in this
401 process. Therefore, unlike the elimination of virus-infected or transformed cells (49),
402 perforin/granzyme-mediated killing is not the essential pathway for the elimination of
403 malaria parasites in the liver. Effector $CD8^+$ T cells were shown herein to form clusters
404 around infected hepatocytes, leading to the elimination of the intra-hepatic parasites.
405 These features suggest that a novel mechanism might be involved in the protective
406 immune responses of $CD8^+$ T cells against intra-hepatic parasites. It is intriguing to
407 speculate that other hepatic immune cells such as dendritic cells, Kupffer cells and liver
408 sinusoidal endothelial cells (43) are involved in parasite elimination.
409

410 Schmidt et al. showed that the proportion of CSP-specific memory $CD8^+$ T cells
411 correlated with sterilizing immunity at the liver stage, with protective effects observed
412 when more than 1% of $CD8^+$ T cells in PBL were CSP-specific (40). In our model, the
413 threshold frequency of OVA-specific memory $CD8^+$ T cells was much higher and
414 required more than 8% OVA-specific $CD8^+$ T cells to achieve sterile immunity in 100%
415 of mice. The probability of sterile immunity was reduced to 28.6% (8/27) when
416 OVA-specific $CD8^+$ T cells constituted 1.1–8.8% of PBL. Therefore, the threshold
417 frequency of memory $CD8^+$ T cells required for the sterile immunity in our OVA system
418 was higher than that in the CSP system. The localization of antigen expression may
419 influence the efficacy and timing of antigen presentation by hepatocytes. CSP is
420 expressed on the surface of the parasite; thus, it may be readily accessible to the
421 cytoplasm of the infected hepatocytes soon after infection. Further, CSP might be
422 transferred to sinusoidal endothelial cells when sporozoites migrate through hepatic
423 sinusoids prior to infection, and these cells cross-present CSP to specific $CD8^+$ T cells in
424 a manner similar to hepatocyte-infecting viruses (50). In contrast, proteins expressed in
425 the cytoplasm of parasites might be transferred to host cells relatively late after infection,

426 and thus may have a narrower window for sterile protection. Alternatively, the outcome
427 of the individual studies may be affected by differences in the mouse strain used (BALB/c
428 for the CSP study and B6 in our OVA study) or the levels of antigen expressed. A recent
429 transcriptome approach revealed that approximately 2,000 genes are active during
430 liver-stage infection (14). It is possible that many of these proteins are expressed in the
431 cytoplasm of parasites and that combined polyclonal $CD8^+$ T cell responses against
432 different sets of these antigens might achieve sterile protection against malaria parasites
433 in the liver.
434
435 Our study showed that malaria proteins expressed in the cytoplasm of parasites can be
436 targets of the protective immune responses by $CD8^+$ T cells. We also visualized the
437 interaction between the infected hepatocytes and specific effector $CD8^+$ T cells, which led
438 to the elimination of the parasites in the liver, and revealed a novel aspect of the effector
439 mechanisms of protective immunity in liver-stage infection. These findings enhance our
440 understanding of the cellular and molecular mechanisms underlying the protective
441 immune responses during the liver stage of malaria infection, and identify novel

candidates for malaria vaccine targets.

444 **ACKNOWLEDGEMENTS**

445 We thank Drs. H. Kosaka and H. Watanabe for providing mice; Drs. Y. Yoshikai and H.

446 Shen for providing LM-OVA; Drs. M. Ishii (Osaka University, Osaka, Japan) and T.

447 Okada (RIKEN Center for Integrative Medical Sciences, Yokohama, Japan) for help in

448 setting up two photon microscopy; and N. Kawamoto for technical assistance. This work

449 was supported by Grants-in-Aid from the Ministry of Education, Science, Sports and

450 Culture, Japan and by Global COE program, Nagasaki University.

451

REFERENCES

1. **Nussenzweig RS, Vanderberg J, Most H, Orton C.** 1967. Protective immunity produced by the injection of X-irradiated sporozoites of *Plasmodium berghei*. Nature **216:**160-162.

2. **Hoffman SL, Doolan DL.** 2000. Malaria vaccines-targeting infected hepatocytes. Nat Med **6:**1218-1219.

3. **Overstreet MG, Cockburn IA, Chen YC, Zavala F.** 2008. Protective CD8 T cells against *Plasmodium* liver stages: immunobiology of an 'unnatural' immune response. Immunol Rev **225:**272-283.

4. **Mueller AK, Labaied M, Kappe SH, Matuschewski K.** 2005. Genetically modified *Plasmodium* parasites as a protective experimental malaria vaccine. Nature **433:**164-167.

5. **Butler NS, Schmidt NW, Vaughan AM, Aly AS, Kappe SH, Harty JT.** 2011. Superior antimalarial immunity after vaccination with late liver stage-arresting genetically attenuated parasites. Cell Host & Microbe **9:**451-462.

6. **Belnoue E, Voza T, Costa FT, Gruner AC, Mauduit M, Rosa DS, Depinay N,**

Kayibanda M, Vigario AM, Mazier D, Snounou G, Sinnis P, Renia L. 2008. Vaccination with live *Plasmodium yoelii* blood stage parasites under chloroquine cover induces cross-stage immunity against malaria liver stage. J Immunol **181:**8552-8558.

7. **Doolan DL, Hoffman SL.** 2000. The complexity of protective immunity against liver-stage malaria. J Immunol **165:**1453-1462.

8. **Rodrigues M, Nussenzweig RS, Zavala F.** 1993. The relative contribution of antibodies, $CD4^+$ and $CD8^+$ T cells to sporozoite-induced protection against malaria. Immunology **80:**1-5.

9. **Good MF, Doolan DL.** 2010. Malaria vaccine design: immunological considerations. Immunity **33:**555-566.

10. **Romero P, Maryanski JL, Corradin G, Nussenzweig RS, Nussenzweig V, Zavala F.** 1989. Cloned cytotoxic T cells recognize an epitope in the circumsporozoite protein and protect against malaria. Nature **341:**323-326.

11. **Hafalla JC, Silvie O, Matuschewski K.** 2011. Cell biology and immunology of malaria. Immunol Rev **240:**297-316.

12. **Kumar KA, Sano G, Boscardin S, Nussenzweig RS, Nussenzweig MC, Zavala F, Nussenzweig V.** 2006. The circumsporozoite protein is an immunodominant protective antigen in irradiated sporozoites. Nature **444:**937-940.

13. **Khusmith S, Charoenvit Y, Kumar S, Sedegah M, Beaudoin RL, Hoffman SL.** 1991. Protection against malaria by vaccination with sporozoite surface protein 2 plus CS protein. Science **252:**715-718.

14. **Rogers WO, Malik A, Mellouk S, Nakamura K, Rogers MD, Szarfman A, Gordon DM, Nussler AK, Aikawa M, Hoffman SL.** 1992. Characterization of *Plasmodium falciparum* sporozoite surface protein 2. Proc Natl Acad Sci U S A **89:**9176-9180.

15. **Wang R, Charoenvit Y, Corradin G, De La Vega P, Franke ED, Hoffman SL.** 1996. Protection against malaria by *Plasmodium yoelii* sporozoite surface protein 2 linear peptide induction of $CD4^+$ T cell- and IFN-γ-dependent elimination of infected hepatocytes. J Immunol **157:**4061-4067.

16. **Weiss WR, Good MF, Hollingdale MR, Miller LH, Berzofsky JA.** 1989. Genetic control of immunity to *Plasmodium yoelii* sporozoites. J Immunol **143:**4263-4266.

17. **Tarun AS, Peng X, Dumpit RF, Ogata Y, Silva-Rivera H, Camargo N, Daly TM, Bergman LW, Kappe SH.** 2008. A combined transcriptome and proteome survey of malaria parasite liver stages. Proc Natl Acad Sci U S A **105:**305-310.

18. **Speake C, Duffy PE.** 2009. Antigens for pre-erythrocytic malaria vaccines: building on success. Parasite Immunol **31:**539-546.

19. **Kaufmann SH, Hess J.** 1999. Impact of intracellular location of and antigen display by intracellular bacteria: implications for vaccine development. Immunology letters **65:**81-84.

20. **Mazzaccaro RJ, Gedde M, Jensen ER, van Santen HM, Ploegh HL, Rock KL, Bloom BR.** 1996. Major histocompatibility class I presentation of soluble antigen facilitated by *Mycobacterium tuberculosis* infection. Proc Natl Acad Sci U S A **93:**11786-11791.

21. **Teitelbaum R, Cammer M, Maitland ML, Freitag NE, Condeelis J, Bloom BR.** 1999. Mycobacterial infection of macrophages results in membrane-permeable phagosomes. Proc Natl Acad Sci U S A **96:**15190-15195.

22. **Garg N, Nunes MP, Tarleton RL.** 1997. Delivery by *Trypanosoma cruzi* of proteins into the MHC class I antigen processing and presentation pathway. J Immunol **158:**3293-3302.

23. **Khan ZM, Ng C, Vanderberg JP.** 1992. Early hepatic stages of *Plasmodium berghei*: release of circumsporozoite protein and host cellular inflammatory response. Infect Immun **60:**264-270.

24. **Hugel FU, Pradel G, Frevert U.** 1996. Release of malaria circumsporozoite protein into the host cell cytoplasm and interaction with ribosomes. Mol Biochem Parasitol **81:**151-170.

25. **Bongfen SE, Torgler R, Romero JF, Renia L, Corradin G.** 2007. *Plasmodium berghei*-infected primary hepatocytes process and present the circumsporozoite protein to specific $CD8^+$ T cells in vitro. J Immunol **178:**7054-7063.

26. **Miyakoda M, Kimura D, Yuda M, Chinzei Y, Shibata Y, Honma K, Yui K.** 2008. Malaria-specific and nonspecific activation of $CD8^+$ T cells during blood stage of *Plasmodium berghei* infection. J Immunol **181:**1420-1428.

27. **Hogquist KA, Jameson SC, Heath WR, Howard JL, Bevan MJ, Carbone FR.** 1994. T cell receptor antagonist peptides induce positive selection. Cell **76:**17-27.

28. **Barnden MJ, Allison J, Heath WR, Carbone FR.** 1998. Defective TCR expression in transgenic mice constructed using cDNA-based α- and β-chain genes under the control of heterologous regulatory elements. Immunol Cell Biol **76:**34-40.

29. **Van Kaer L, Ashton-Rickardt PG, Ploegh HL, Tonegawa S.** 1992. TAP1 mutant mice are deficient in antigen presentation, surface class I molecules, and $CD4^-8^+$ T cells. Cell **71:**1205-1214.

30. **Kawabata Y, Udono H, Honma K, Ueda M, Mukae H, Kadota J, Kohno S, Yui K.** 2002. Merozoite surface protein 1-specific immune response is protective against exoerythrocytic forms of *Plasmodium yoelii*. Infect Immun **70:**6075-6082.

31. **Ishino T, Yano K, Chinzei Y, Yuda M.** 2004. Cell-passage activity is required for the malarial parasite to cross the liver sinusoidal cell layer. PLoS biology **2:**E4.

32. **Badovinac VP, Messingham KA, Jabbari A, Haring JS, Harty JT.** 2005. Accelerated $CD8^+$ T-cell memory and prime-boost response after dendritic-cell vaccination. Nat Med **11:**748-756.

33. **Dudani R, Chapdelaine Y, Faassen Hv H, Smith DK, Shen H, Krishnan L, Sad S.** 2002. Multiple mechanisms compensate to enhance tumor-protective $CD8^+$ T cell response in the long-term despite poor $CD8^+$ T cell priming initially: comparison between an acute versus a chronic intracellular bacterium expressing a model antigen. J Immunol **168:**5737-5745.

34. **Udono H, Yamano T, Kawabata Y, Ueda M, Yui K.** 2001. Generation of cytotoxic T lymphocytes by MHC class I ligands fused to heat shock cognate protein 70. Int Immunol **13:**1233-1242.

35. **Huang Q, Richmond JF, Suzue K, Eisen HN, Young RA.** 2000. In vivo cytotoxic T lymphocyte elicitation by mycobacterial heat shock protein 70 fusion

proteins maps to a discrete domain and is $CD4^+$ T cell independent. J Exp Med **191:**403-408.

36. **Gruring C, Heiber A, Kruse F, Ungefehr J, Gilberger TW, Spielmann T.** 2011. Development and host cell modifications of *Plasmodium falciparum* blood stages in four dimensions. Nat Commun **2:**165.

37. **Sano G, Hafalla JC, Morrot A, Abe R, Lafaille JJ, Zavala F.** 2001. Swift development of protective effector functions in naive $CD8^+$ T cells against malaria liver stages. J Exp Med **194:**173-180.

38. **Rai D, Pham NL, Harty JT, Badovinac VP.** 2009. Tracking the total CD8 T cell response to infection reveals substantial discordance in magnitude and kinetics between inbred and outbred hosts. J Immunol **183:**7672-7681.

39. **Cockburn IA, Tse SW, Radtke AJ, Srinivasan P, Chen YC, Sinnis P, Zavala F.** 2011. Dendritic cells and hepatocytes use distinct pathways to process protective antigen from plasmodium in vivo. PLoS Pathog **7:**e1001318.

40. **Schmidt NW, Podyminogin RL, Butler NS, Badovinac VP, Tucker BJ, Bahjat KS, Lauer P, Reyes-Sandoval A, Hutchings CL, Moore AC, Gilbert**

SC, Hill AV, Bartholomay LC, Harty JT. 2008. Memory CD8 T cell responses exceeding a large but definable threshold provide long-term immunity to malaria. Proc Natl Acad Sci U S A **105:**14017-14022.

41. **Sturm A, Amino R, van de Sand C, Regen T, Retzlaff S, Rennenberg A, Krueger A, Pollok JM, Menard R, Heussler VT.** 2006. Manipulation of host hepatocytes by the malaria parasite for delivery into liver sinusoids. Science **313:**1287-1290.

42. **Amino R, Thiberge S, Martin B, Celli S, Shorte S, Frischknecht F, Menard R.** 2006. Quantitative imaging of *Plasmodium* transmission from mosquito to mammal. Nat Med **12:**220-224.

43. **Frevert U, Nardin E.** 2008. Cellular effector mechanisms against *Plasmodium* liver stages. Cell Microbiol **10:**1956-1967.

44. **Cockburn IA, Amino R, Kelemen RK, Kuo SC, Tse SW, Radtke A, Mac-Daniel L, Ganusov VV, Zavala F, Menard R.** 2013. In vivo imaging of $CD8^+$ T cell-mediated elimination of malaria liver stages. Proc Natl Acad Sci U S A **110:**9090-9095.

45. **Renggli J, Hahne M, Matile H, Betschart B, Tschopp J, Corradin G.** 1997. Elimination of P. berghei liver stages is independent of Fas (CD95/Apo-I) or perforin-mediated cytotoxicity. Parasite Immunol **19:**145-148.

46. **Chakravarty S, Baldeviano GC, Overstreet MG, Zavala F.** 2008. Effector $CD8^+$ T lymphocytes against liver stages of *Plasmodium yoelii* do not require γ interferon for antiparasite activity. Infect Immun **76:**3628-3631.

47. **Butler NS, Schmidt NW, Harty JT.** 2010. Differential effector pathways regulate memory CD8 T cell immunity against *Plasmodium berghei* versus *P. yoelii* sporozoites. J Immunol **184:**2528-2538.

48. **Trimnell A, Takagi A, Gupta M, Richie TL, Kappe SH, Wang R.** 2009. Genetically attenuated parasite vaccines induce contact-dependent $CD8^+$ T cell killing of *Plasmodium yoelii* liver stage-infected hepatocytes. J Immunol **183:**5870-5878.

49. **Trapani JA, Smyth MJ.** 2002. Functional significance of the perforin/granzyme cell death pathway. Nature Rev Immunol **2:**735-747.

50. **Wohlleber D, Kashkar H, Gartner K, Frings MK, Odenthal M, Hegenbarth S, Borner C, Arnold B, Hammerling G, Nieswandt B, van Rooijen N, Limmer A, Cederbrant K, Heikenwalder M, Pasparakis M, Protzer U, Dienes HP, Kurts C, Kronke M, Knolle PA.** 2012. TNF-induced target cell killing by CTL activated through cross-presentation. Cell reports **2:**478-487.

FIGURE LEGENDS

Figure 1

The expression of a model antigen in the cytoplasm of recombinant PbA.

(A) Schematic representation of the transgenic PbA constructs used in this study. (B) PbA-gfpOVA sporozoites, HepG2 cells infected with PbA-gfpOVA sporozoites *in vitro*, and infected RBCs (iRBC) were stained with Bodipy-TR-C_5-ceratide and DRAQ5, which mark membrane structure and nuclei, respectively. Images were obtained using confocal microscopy. Arrowheads indicate the margin of the RBC, and the scale bars indicate 5 μm.

Figure 2

OT-I cells protect against infection with sporozoites of OVA-expressing PbA.

B6 mice were inoculated with activated OT-I $CD8^+$ T cells ($0–10^7$) (A, B) and infected with sporozoites (300/mouse) of PbA-hsOVA, wild-type PbA (A), or PbA-gfpOVA (B) 2 days later. Alternatively, after transfer with OT-II $CD4^+$ T cells (3×10^7 or 0), mice were infected with PbA-hsOVA sporozoites (500/mouse) (C). Representative flow cytometry

profiles of PBLs from mice transferred with OT-I cells (1×10^7) (A, B) or OT-II cells (3×10^7) (C) are shown. The proportion of OT-I or OT-II cells within the total $CD8^+$ or $CD4^+$ T cell populations are indicated. Note that the levels of CD8 expression on activated T cells are reduced as reported previously (38). The number in the upper left of each graph indicates the number of transferred cells; the number in parentheses indicates the proportion of OT-I cells in the total $CD8^+$ T cell population in PBL at the time of infection. Parasitemia was monitored daily starting 4 days after infection. Values significantly different ($p < 0.05$) from mice not receiving T cells are indicated (*). The experiments were performed twice (B, C) or 3 times (A); representative data are shown.

Figure 3

TAP-dependent presentation of MHC I epitope by infected host cells.

B6 or $TAP^{-/-}$ mice were inoculated (or not inoculated, for controls) with activated OT-I $CD8^+$ T cells and infected with sporozoites (5×10^3) of PbA-hsOVA or PbA (A, B). The numbers in parentheses indicate the proportion of OT-I cells in the total $CD8^+$ T cell population in PBL at the time of infection (A). Bone marrow (BM) chimeras were generated between B6 and $TAP^{-/-}$ mice (as described in the Materials and Methods section), inoculated with OT-I cells, and infected with PbA-hsOVA sporozoites (C). Two

days after infection, RNA was extracted from the liver of the infected mice, and parasite burden was determined by real-time PCR. The experiments were performed twice (A) or 3 times (B, C); representative data are shown. ns, not significant; *, $p < 0.05$; **, $p < 0.01$.

Figure 4

Clustering of OT-I cells around GFP$^+$ infected hepatocytes during liver-stage infection with PbA-gfpOVA

B6 mice were transferred with activated DsRed/OT-I CD8$^+$ T cells at a dose of 3×10^6 (A, C, D, F) or 1×10^7 (B, C-F), and were infected with PbA-gfpOVA sporozoites (1×10^4). Some mice did not receive DsRed/OT-I or were not infected with PbA-gfpOVA as controls (E, F). Forty-eight hours after infection, the liver was imaged with TPM. The 2 dimensional projections of 3 dimensional imaging volumes are shown, and the scale bars indicate 10 μm (A, B). A still image of GFP$^+$ cell disappearance while in contact with OT-I cells is shown (A, right image; time-lapse image in supplementary Fig. 1). The numbers of GFP$^+$ cells and T-cell clusters were counted within a surface area of 75mm^2 using fluorescence microscopy (C, E). GFP$^+$ cells and T-cell clusters were imaged in 3 dimensions using TPM, and the number of OT-I cells within each cluster was determined

using Imaris software (D, F). The number of OT-I cells were determined separately for clusters containing and not containing GFP^+ cells (D). Bars indicate average. *, $p < 0.05$; **, $p < 0.01$; ***, $p < 0.0001$.

Figure 5

Perforin and IFN-γ expressed in $CD8^+$ T cells are dispensable for sterile immunity at the liver stage of infection.

Activated $CD8^+$ T cells from perforin$^{-/-}$IFN-$\gamma^{-/-}$ OT-I, IFN-$\gamma^{-/-}$ OT-I, perforin$^{-/-}$ OT-I, wild-type OT-I mice, or no cells (-) were adoptively transferred into B6 mice, which were then infected with sporozoites (300/mouse) of PbA-hsOVA (A) or PbA-gfpOVA (B), and the levels of parasitemia were monitored. Values significantly different ($p < 0.05$) from mice not receiving OT-I cells are indicated (*). In each graph, the number in parentheses indicates the proportion of OT-I cells in the total $CD8^+$ T cell population in PBL at the time of infection. The experiments were performed 3 times; representative data are shown.

Figure 6

OVA-specific memory $CD8^+$ T cells were protective against infection with PbA-hsOVA.

B6 mice were immunized with $OVA_{257-264}$ as described in the Materials and Methods section. Two months later, the proportion of OVA-specific memory $CD8^+$ T cells was determined by staining PBL with anti-CD8 mAb and $OVA_{257-264}$/H-$2K^b$ tetramer. Representative flow cytometry profiles of PBLs from naive and immunized mice are shown (A). Each bar in the graph shows the proportion of OVA-specific memory $CD8^+$ T cells in total $CD8^+$ T cells for an individual mouse (left axis) (B). The data are arranged from left to right in order of high to low specific $CD8^+$ T cell ratios. These mice were challenged by intravenous injection of PbA-hsOVA sporozoites (1,000/mouse). Parasitemia was assessed 8 days after challenge; each dot shows the level of parasitemia in an individual mouse (right axis). Data from 37 mice are summarized in (C). * < 0.05%. The experiments were performed 3 times; pooled data are shown.

Figure 1

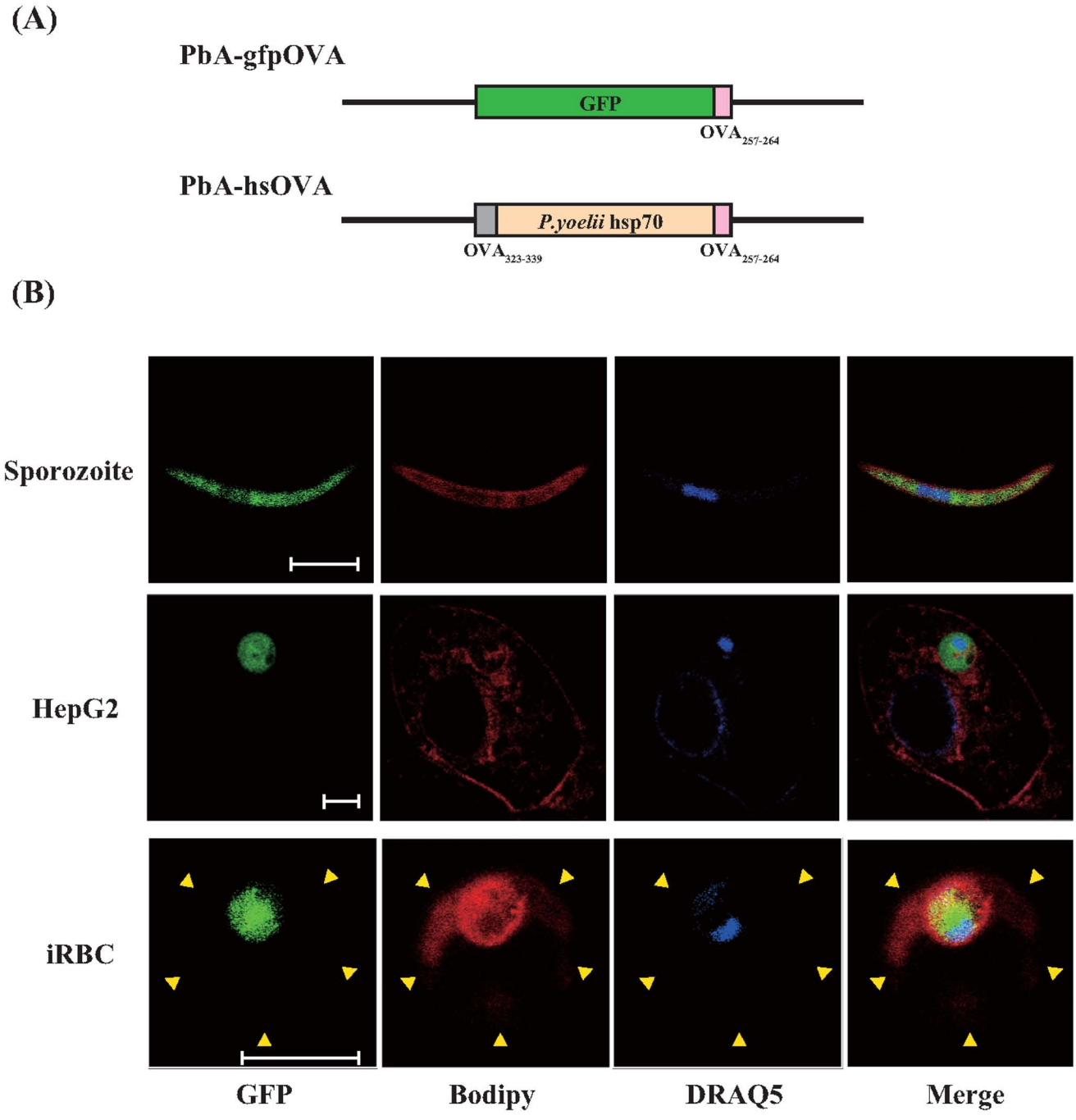
(A)
PbA-gfpOVA
GFP
OVA257-264
PbA-hsOVA
P.yoelii hsp70
OVA323-339
OVA257-264
(B)
Sporozoite
HepG2
iRBC
GFP
Bodipy
DRAQ5
Merge

Figure 2

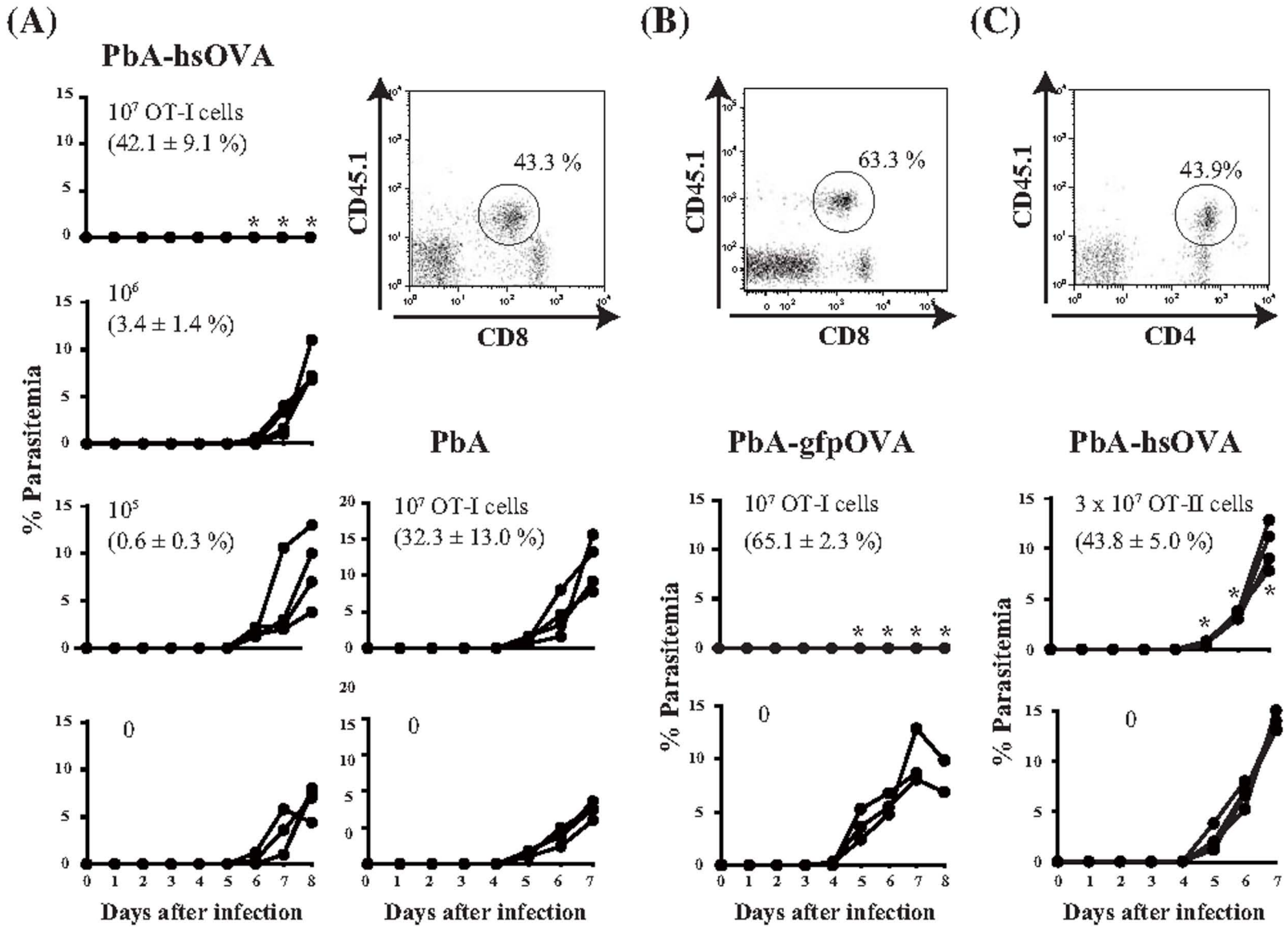
(A)
PbA-hsOVA
10⁷ OT-I cells
(42.1 ± 9.1 %)
10⁶
(3.4 ± 1.4 %)
10⁵
(0.6 ± 0.3 %)
0
% Parasitemia
Days after infection
CD45.1
CD8
43.3 %
PbA
10⁷ OT-I cells
(32.3 ± 13.0 %)
0
Days after infection
(B)
63.3 %
PbA-gfpOVA
10⁷ OT-I cells
(65.1 ± 2.3 %)
0
% Parasitemia
Days after infection
(C)
CD4
43.9%
PbA-hsOVA
3 x 10⁷ OT-II cells
(43.8 ± 5.0 %)
0
% Parasitemia
Days after infection

Figure 3

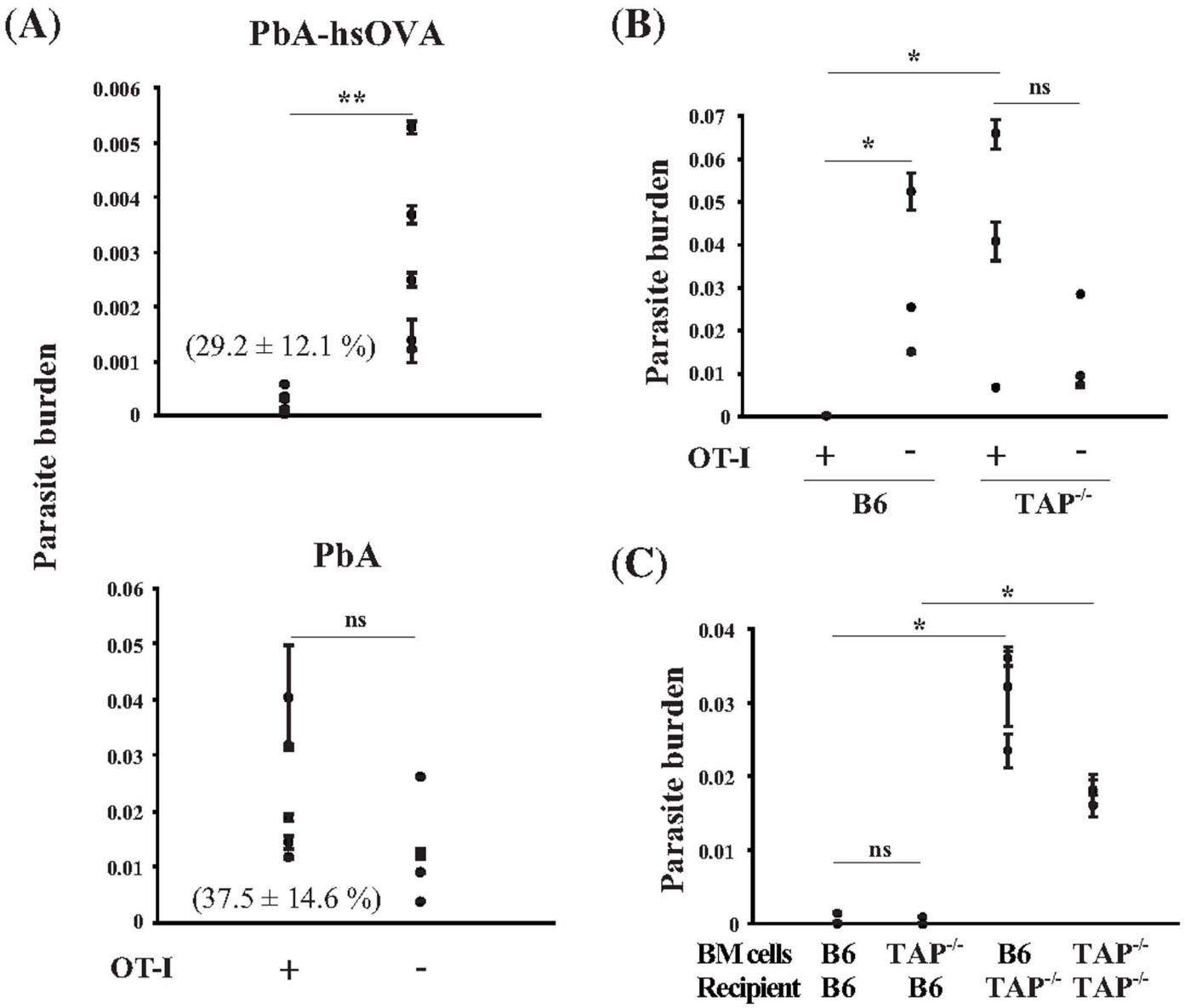
(A)
PbA-hsOVA
Parasite burden
0.006
0.005
0.004
0.003
0.002
0.001
0
**
(29.2 ± 12.1 %)
PbA
0.06
0.05
0.04
0.03
0.02
0.01
0
ns
(37.5 ± 14.6 %)
OT-I
+
-
(B)
Parasite burden
0.07
0.06
0.05
0.04
0.03
0.02
0.01
0
*
*
ns
OT-I
+
-
+
-
B6
TAP-/-
(C)
Parasite burden
0.04
0.03
0.02
0.01
0
*
*
ns
BM cells
B6
TAP-/-
B6
TAP-/-
Recipient
B6
B6
TAP-/-
TAP-/-

Figure 4

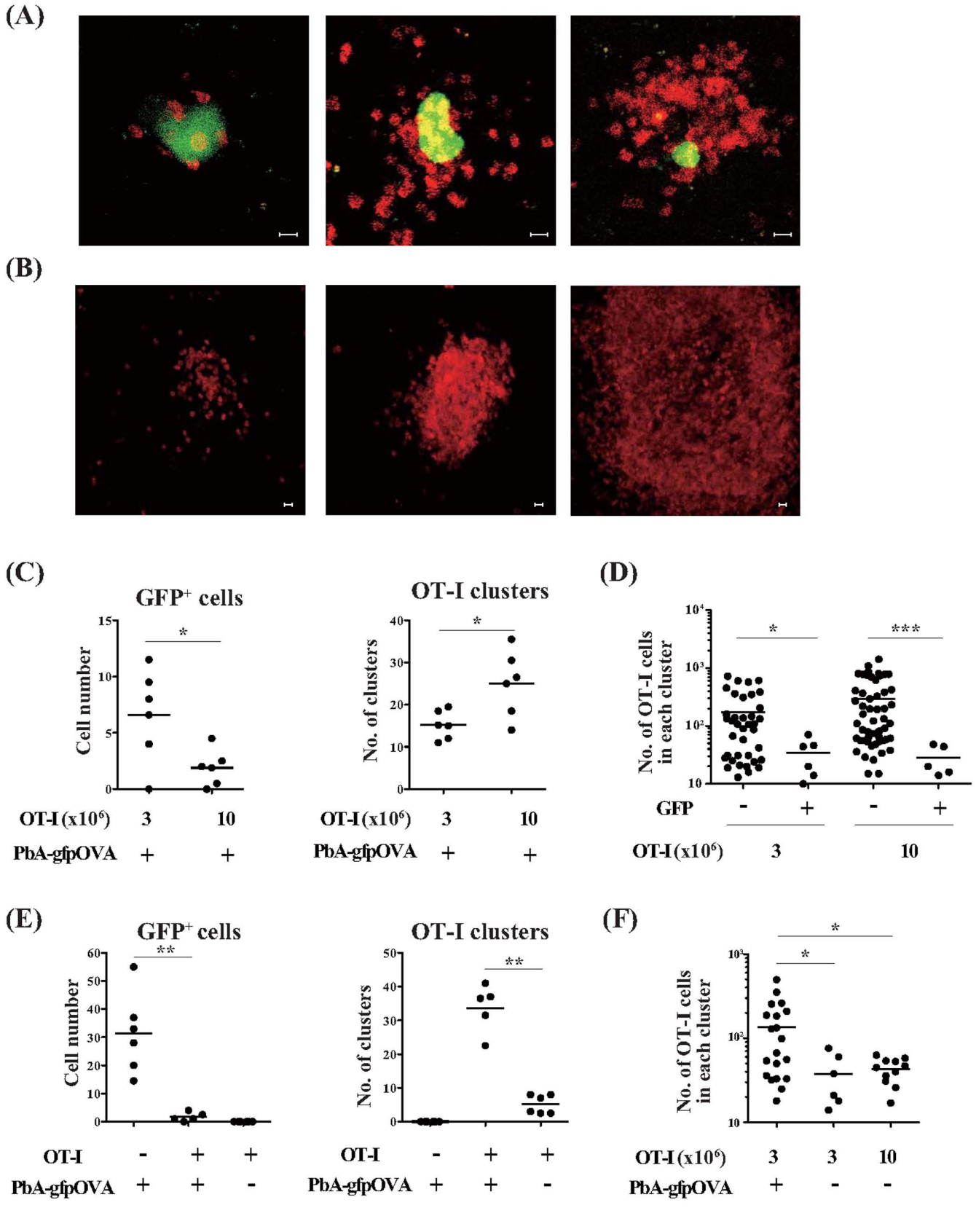
(A)
(B)
(C)
GFP+ cells
Cell number
OT-I clusters
No. of clusters
OT-I (x10⁶) 3 10
PbA-gfpOVA + +
(D)
No. of OT-I cells in each cluster
GFP - + - +
OT-I (x10⁶) 3 10
(E)
GFP+ cells
Cell number
OT-I clusters
No. of clusters
OT-I - + +
PbA-gfpOVA + + -
(F)
No. of OT-I cells in each cluster
OT-I (x10⁶) 3 3 10
PbA-gfpOVA + - -

Figure 5

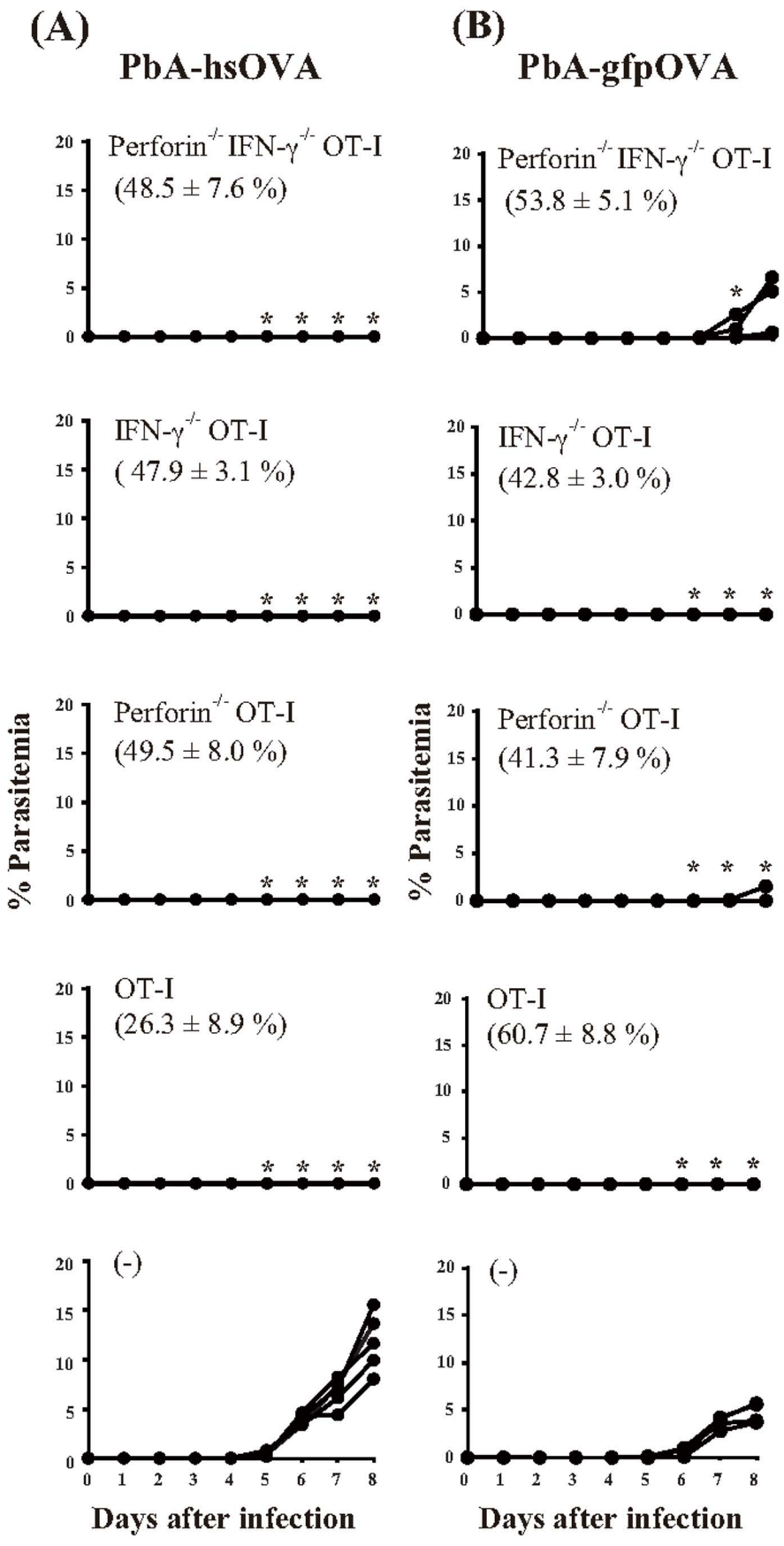
(A)
PbA-hsOVA
(B)
PbA-gfpOVA
Perforin-/- IFN-γ-/- OT-I
(48.5 ± 7.6 %)
Perforin-/- IFN-γ-/- OT-I
(53.8 ± 5.1 %)
IFN-γ-/- OT-I
(47.9 ± 3.1 %)
IFN-γ-/- OT-I
(42.8 ± 3.0 %)
Perforin-/- OT-I
(49.5 ± 8.0 %)
Perforin-/- OT-I
(41.3 ± 7.9 %)
% Parasitemia
% Parasitemia
OT-I
(26.3 ± 8.9 %)
OT-I
(60.7 ± 8.8 %)
(-)
(-)
0 1 2 3 4 5 6 7 8
Days after infection
Days after infection

Figure 6

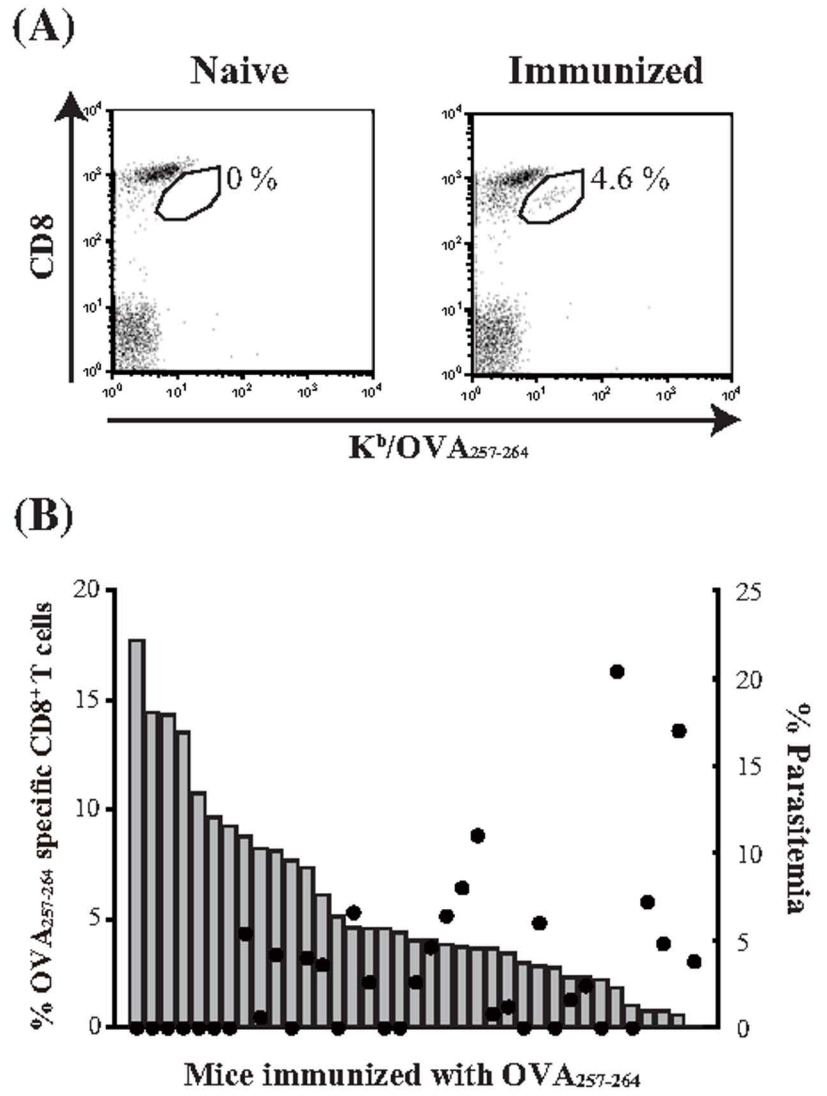

(C)

% $OVA_{257-264}$ specific $CD8^+$ T cells	Challenged	Protected	% Protected
>8.8	7	7	100 *
8.8~1.1	26	8	30.8 *
<1.1	4	0	0